actuators

Article

Model-Free-Based Single-Dimension Fuzzy SMC Design for Underactuated Quadrotor UAV

Ghulam E Mustafa Abro [1,*], Saiful Azrin B. M. Zulkifli [1], Vijanth Sagayan Asirvadam [1] and Zain Anwar Ali [2]

1 Department of Electrical & Electronic Engineering, Universiti Teknologi PETRONAS, Seri Iskandar 32610, Malaysia; saifulazrin_mz@utp.edu.my (S.A.B.M.Z.); vijanth_sagayan@utp.edu.my (V.S.A.)
2 School of Systems Science, Beijing Normal University, Beijing 100875, China; Zainanwar86@bnu.edu.cn
* Correspondence: Ghulam_20000150@utp.edu.my

Abstract: The underactuated quadrotor unmanned aerial vehicle (UAV) is one of the nonlinear systems that have few actuators as compared to the degree of freedom (DOF); thus, it is a strenuous task to stabilize its attitude and positions. Moreover, an induction of unmodelled dynamic factors and uncertainties make it more difficult to control its maneuverability. In this paper, a model-free based single-dimension fuzzy sliding mode control (MFSDF-SMC) is proposed to control the attitude and positions of underactuated quadrotor UAV. The paper discusses the kinematic and dynamic models with unmodelled dynamic factors and unknown external disturbances. These unmodelled factors and disturbances may lead the quadrotor towards failure in tracking specific trajectory and may also generate some serious transient and steady-state issues. Furthermore, to avoid the problem of gimbal lock, the model is amalgamated with hyperbolic function to resolve the singularity issues dully developed due to Newton Euler's dynamic modeling. The simulation results performed for MFSDF-SMC using MATLAB software R2020a are compared with conventional sliding mode control, fuzzy-based sliding control and single-dimension fuzzy-based sliding mode control without a model-free approach. The design and implementation of the model-free single dimension-based fuzzy sliding mode control (MFSDF-SMC) with an updated Lyapunov stability theorem is presented in this work. It is observed that MFSDF-SMC produces robust trajectory performance therefore, and the manuscript suggests the experimental setup to test the proposed algorithm in a noisy environment keeping the same conditions. The verification of the equipment used and its effective demonstration is also available for the reader within the manuscript.

Keywords: model-free approach; quadrotor; single-dimension fuzzy; sliding mode control; unmodelled dynamics; underactuated system

check for updates

Citation: Abro, G.E.M.; Zulkifli, S.A.B.M.; Asirvadam, V.S.; Ali, Z.A. Model-Free-Based Single-Dimension Fuzzy SMC Design for Underactuated Quadrotor UAV. *Actuators* **2021**, *10*, 191. https://doi.org/10.3390/act10080191

Academic Editor: Hai Wang

Received: 7 May 2021
Accepted: 11 June 2021
Published: 10 August 2021

1. Introduction

Underactuated quadrotors are a type of unmanned aerial vehicles (UAVs) that have fewer control inputs or actuators than the degree of freedom (DOF). Due to this reason, they are difficult to stabilize but on the other hand they consume much less power and may exhibit natural dynamic motion if controlled properly. Thus, this is one of the main reasons that researchers are still evaluating the capability and flexibility of quadrotor UAV in various modes, i.e., trajectory tracking, hovering, vertical take-off, and landing (VTOL). In the modern world, one may witness the utilization of such underactuated quadrotor UAVs in military as well as in civil vicinities.

As per the construction point of view, it has four brushless DC (BLDC) motors dully controlled via electronic speed controller (ESC). One with ESC can control the speed of BLDC motors in a precise way, and this is the main reason for proposing it in this research work. There have been various control strategies [1,2] to produce the robust response and several observer designs [3] to observe and estimate unmodelled dynamic factors and unknown external disturbances, but still there are some limitations as discussed in [3]. In addition to this, one may see various model-based control designs, i.e., linearized model-based control strategies [4–10] and nonlinear model-based control techniques [11–18]. The fuzzy-logic-based self-tuning of proportional integral derivative (F-PID) control is proposed for attitude and position control with the linear dynamic model [4,5]. In this scheme, the gains of proportional integral and derivative (PID) are tuned to acquire the robust performance. Researchers have proposed Kalman filter scheme to estimate the attitude with different data sets acquired from the inertial measurement unit (IMU) [6]. One may also see the different configurations of proportional (P), integral (I), and derivative (D), in either cascaded or parallel form. The double-gain PD scheme is also proposed for regulating linear attitude dynamics [6]. Similar linear dynamic model is opted in [7], where a linear-quadratic and regulator (LQR) controller is designed with full-state linear observer design. In the previous proposed research works, the sliding mode control (SMC) technique was applied to improve the same attitude and positions of underactuated quadrotor but with linear Newton Euler dynamics [8]. One may see the trend of hybridizing these control and observer design schemes with adaptive techniques to overcome the parametric uncertainties and unmodelled dynamic factors [9]. So far, researchers have proposed various strategies to acquire more realistic real-world dynamic models such as using a continuous predictor-based identification approach. This approach uses the matrix inequality concept for tuning the gains for an underactuated quadrotor [10]. The stability is achieved in all these control algorithms but around the equilibrium conditions using Jacobian method. Thus, researchers later consider the nonlinear models. The idea behind the proposition of this intelligent control algorithm with a model-free approach is to achieve a minimum chattering effect, reduce the delay in all angular and translational accelerations, and minimize transient and steady-state issues, i.e., steady-state error, overshoots and settling time, even in the presence of unmodelled dynamic factors and external disturbances [3].

The subject is introduced in Section 1. Section 2 briefs the reader about the previous research contributions. Section 3 presents the study of an underactuated quadrotor dynamic model with unmodelled dynamic factors and unknown external disturbances. Furthermore, the Section 4 demonstrates the proposed model-free single-dimension fuzzy-based sliding mode control (MFSDF-SMC) along with its stability proof using Lyapunov stability theorem. Section 5 shares the software simulations and analysis among the SMC, conventional fuzzy-based SMC, and single-dimension fuzzy-based sliding mode control design with and without model-free approach. The hardware configuration and experimental results can be seen in Section 6, and last but not the least the entire research finding is concluded in Section 7.

2. Literature Review

There are number of research contributions where nonlinear dynamic model of an underactuated quadrotor craft is considered. Researchers proposed several control designs such as sliding mode control (SMC) and backstepping control (BSC) [11,12] for stabilizing the attitude and positions during the flight mode. These techniques only focused on bounded values for unmodeled dynamic factors and external disturbances [13]. Researchers have also provided comparative study for evaluating the performance of PD control for linear and nonlinear dynamic model of quadrotor in hovering position [14]. Researchers have designed some of the algorithms that provide robust results, i.e., comparatively better convergence rate within finite time [15]. To improve tracking performances, one may find number of nonlinear model-based control designs [16–19], whereas for robust control designs, they really need complete information about the system, and therefore the system requires lots of sensors and mainly one inertial measurement unit (IMU). Most of the schemes are based on Newton Euler dynamic models. A robust backstepping integral sliding mode control is proposed for the trajectory control of an underactuated and nonlinear quadrotor craft. In the proposed technique [20], one may see the approach is applied on a dynamic model that is derived using Newton Euler method leading to gimbal lock issue again. In addition to this, position errors are also observed. A gain-scheduled proportional integral derivative (G-PID) is proposed in [21] for robust tracking performance, but some overshoots along with steady-state error occurred.

The controllers such as linear quadratic regulator (LQR) and PID are mostly applied to achieve better performance, but for the case of underactuated quadrotor in the presence of unmodelled dynamics, these schemes have several performance issues such as slow convergence rate, gimbal lock and transient and steady-state issues [22]. These unmodelled dynamic factors were previously considered one by one, where aerodynamic effects were addressed using integral backstepping control law and then using fractional order backstepping sliding mode controller. These schemes were not only sensitive to disturbances but also to producing high-frequency oscillations known as chattering effect (number of high oscillations on rotors) [23,24]. It is quite clear that for proposing an intelligent control design or observer-based control, one should derive the accurate dynamic model considering all other unmodelled dynamic factors. This is one of the complex tasks, and thus it demands either more precise model derivation or more precise experiments [25]. These problems are addressed later using higher-order sliding mode control laws such as demonstrated in [26,27]. It is an admitted fact that the Euler angles are strongly coupled to each other; hence, to invert the control inputs in object-oriented design to get the loose coupling is known as inversion control algorithm as seen in [28]. Researchers have proposed various combinations of inversion control to stabilize the quadrotor. In [29], a nonlinear dynamic inversion control law has been observed where it is developed to address the coupling issue [30–32]. For the model, the inertial and unmodelled dynamics are very difficult and can affect the UAV at same time. Therefore, researchers have used Lyapunov theorem in many papers for the stability proof. Such types of control laws and schemes can be visualized in [33].

Simply, it is not an issue of intelligent control designs, but a serious concern related to dynamic model of the unmanned aerial vehicles (UAVs). Since the paper is focused on an underactuated quadrotor craft, it considers these factors within the Newton Euler dynamic model along with hyperbolic function to address the singularity issue (Gimbal Lock). The precise mathematical model for underactuated quadrotor unmanned aerial vehicle is difficult because of several types of time-varying parameters that instantaneously change, such as wind disturbance, the payload mass variation (smooth and non-smooth), the chattering effect and other external disturbances. To address this issue, researchers have proposed model-free control techniques to control and stabilize the system. Researchers have proposed different versions such as piecewise recursive approach [34–36], time delay estimation control design [37], algebraic method-oriented hybrid PID control designs [38–40] and many more.

This manuscript proposes a model-free single-dimension fuzzy-based sliding mode control (SDF-SMC) design. The technique of single-dimension fuzzy-based sliding mode control has been proposed previously without model-free approach for several applications such as deep submergence rescue vehicle (DSRV) [41], double pendulum-type overhead crane [42] and NPS AUV II [43] for Pantograph-Cateary system [44] and for underactuated quadrotor craft [45]. This algorithm produced many methods, such as fast convergence rate, prompt execution time response, less chattering effect and less control input energy (CIE). The output response of SDF-SMC in all research contributions produces sound results until the induction of external disturbances and unmodelled dynamic factors. In contrast with fuzzy-based control design [46], artificial neural network and genetic algorithm [47,48], SMC is the better control technique for such underactuated systems. The only limitation is its high sensitivity to unmodelled dynamic factors and disturbances, which results in it generating high number of oscillations due to sliding surface [49].

This section shows that sliding mode control has many more perks than other control designs. It has one issue of chattering phenomenon, which is high number of oscillations that appear on four rotors of underactuated quadrotor [50]. Researchers have hybridized SMC with fuzzy logic control (FLC) [51] to improve the performance and reduce the chattering or Zeno phenomenon. The only issue with this control strategy is consumption of huge computational time, bandwidth and power source. This is all because of its several sub-stages such as fuzzification, inference of rules and lastly the defuzzification stage, whereas the intelligent algorithms as mentioned in [52] are not recommended because they do not facilitate the quadrotor in real-time self-tuning of the gains or the improvement of impulsive behavior [53,54]. Similarly, if one discusses the fuzzy H∞ output feedback control then its output is also quantized and therefore either introduces the chattering noise or provides some delay [55,56]. This manuscript proposes sliding mode control design with an adaptive flavor. This combines the SMC with an improved version of Fuzzy logic control to acquire the maximum computational speed with maximum efficiency and of course enough capability to tackle the unmodelled dynamic factors and external disturbances. This technique is named the model-free single-dimension fuzzy-based sliding mode control (MFSDF-SMC). By doing this, the chattering phenomenon will be reduced comparatively from the responses and the quadrotor will be able to perform the aggressive maneuvers. Novelty of this approach is that it ensures the stability and tracking under any uncertainty that is created due to unmodelled dynamic factors and unknown external disturbances. This model-free approach will ensure the bounded tracking errors, whereas the single-dimension fuzzy-based sliding mode control will try to stabilize the underactuated system by eliminating the bounded error in a finite time. In addition to this, MFSDF-SMC will also reduce the computational time and control input energy so that the quadrotor can play aggressive operations.

3. Mathematical Model

Underactuated quadrotor is one of the nonlinear unstable systems and comprises four brushless DC (BLDC) motors whose thrust is treated as an input to entire system. There are several factors that one must consider while deriving the dynamic model of underactuated quadrotor. These factors are thrust force generated via the rotation of propellers, torque, gravity component and gyroscopic factors. To derive the dynamic model using Newton Euler dynamics, one must consider the body frame of quadrotor as a rigid and symmetrical structure as one of the assumptions to derive appropriate dynamics.

Table 1 shows all the symbols along with their description. The change in the underactuated quadrotor's attitude is indicated by roll, pitch, and yaw angles, which are denoted as φ, θ and ψ. These are obtained relatively to the x-, y- and z-axes. Moreover, one may see some of the nearer and appropriate dynamical models for quadrotor in [57,58]. Research contributions such as in [59,60] exist, where researchers derived the Euler-lagrange technique to acquire the dynamics for underactuated quadrotor craft. Moreover, in the Equations (1)–(6), $u_1 = \mathrm{T}_2 - \mathrm{T}_4 = k_{\mathrm{thr}} \cdot \left(\Omega_2^2 - \Omega_4^2\right)$, $u_2 = \mathrm{T}_1 - \mathrm{T}_3 = k_{\mathrm{thr}} \cdot \left(\Omega_1^2 - \Omega_3^2\right)$, $u_3 = b_{\mathrm{dragg}} \cdot \left(\Omega_1^2 - \Omega_2^2 + \Omega_3^2 - \Omega_4^2\right)$ and $u_4 = \sum_{\mathrm{l}=1}^{4} \mathrm{F_i} = \sum_{\mathrm{l}=1}^{4} \mathrm{T_i}$. This $\mathrm{T_i} = \mathrm{T}_1 + \mathrm{T}_2 + \mathrm{T}_3 + \mathrm{T}_4$ whereas Ω is given as the sum = $-\Omega_1 + \Omega_2 - \Omega_3 + \Omega_4$.

$$\ddot{\varphi} = \left(lu_1 - \dot{I}_{xx}\dot{\varphi}\right)/I_{xx} \tag{1}$$

$$\ddot{\theta} = \left(lu_2 - \dot{I}_{yy}\dot{\theta}\right)/I_{yy} \tag{2}$$

$$\ddot{\psi} = \left(lu_3 - \dot{I}_{zz}\dot{\psi}\right)/I_{zz} \tag{3}$$

$$\ddot{x} = -u_4 \sin\theta/m \tag{4}$$

$$\ddot{y} = u_4 \sin\varphi \cos\theta/m \tag{5}$$

$$\ddot{z} = u_4 \cos\varphi \cos\theta/(m-g) \tag{6}$$

Table 1. Symbols with their brief description and Units.

Symbols	Unit	Description
M	Kg	Mass of underactuated quadrotor
G	m/s^2	Gravitational force
L	M	Length of underactuated quadrotor's arm
R		Rotational matrix
K_{thr}	ms^2	Thrust component
B_{DRAGG}	Nms^2	Dragging component
Ω_I	Rev/min	Rotation rate of propeller fans
J_R		Inertia of rotor
T_I	N	Thrust created by each BLDC motor
F_I	N	Forces in the respective directions
D_I		Time depended on disturbances
I_{XX}		Inertia at *x*-axis
I_{YY}		Inertia at *y*-axis
I_{ZZ}		Inertia at z-axis
$\Delta\phi$, $\Delta\theta$, *and* $\Delta\psi$		Unmodelled system dynamics

The equation set (1) to (6) is derived via Euler lagrange method, and it does not consider quadrotor as nonlinear system with very strong coupled factors. Thus, the dynamic model of underactuated quadrotor is derived using Newton Euler dynamic approach in [61] as given below:

$$\ddot{\phi} = \frac{I_{yy} - I_{zz}}{I_{xx}}\dot{\theta}\dot{\psi} + \frac{l}{I_{xx}}u_1 \tag{7}$$

$$\ddot{\theta} = \frac{I_{zz} - I_{xx}}{I_{yy}}\dot{\phi}\dot{\psi} + \frac{l}{I_{yy}}u_2 \tag{8}$$

$$\ddot{\psi} = \frac{I_{xx} - I_{yy}}{I_{zz}}\dot{\phi}\dot{\theta} + \frac{l}{I_{zz}}u_3 \tag{9}$$

$$\ddot{x} = (u_4 u_x)/m \tag{10}$$

$$\ddot{y} = (u_4 u_y)/m \tag{11}$$

$$\ddot{z} = (u_4 \cos\varphi \cos\theta - mg)/m \tag{12}$$

Moreover, in the equation set from (7) to (12), $u_1 = \mathrm{T}_2 - \mathrm{T}_4$, $u_2 = \mathrm{T}_1 - \mathrm{T}_3$, $u_3 = T_1 + T_3 - T_2 - T_4$ and $u_\mathrm{x} = \sin\psi \sin\theta \cos\varphi$, $u_\mathrm{y} = \sin\psi \sin\theta \cos\varphi - \cos\psi \sin\varphi$ and $u_4 = \sum_{\mathrm{l}=1}^{4} \mathrm{F_i} = \sum_{\mathrm{l}=1}^{4} \mathrm{T_i}$. This $\mathrm{T_i} = \mathrm{T}_1 + \mathrm{T}_2 + \mathrm{T}_3 + \mathrm{T}_4$. The shortcoming of this model is the ignorance of the torque factor that is produced by the revolutions of rotors during flight. To consider this one of the major factors, here we add $-J_r\dot{\theta}\Omega/I_{xx}$ and $J_r\dot{\theta}\Omega/I_{yy}$ [62–64]. By adding this, one may see the effect of unmodelled dynamics in acquired model as mentioned in the following set of equations:

$$\dot{\phi} = a_1\dot{\theta}\dot{\psi} + c_1\dot{\theta}\Omega + d_1 + b_1 u_1 \tag{13}$$

$$\ddot{\theta} = a_2\dot{\phi}\dot{\psi} + c_2\dot{\phi}\Omega + d_2 + b_2 u_2 \tag{14}$$

$$\ddot{\psi} = a_3\dot{\phi}\dot{\theta} + d_3 + b_3 u_3 \tag{15}$$

$$\ddot{x} = (u_4\ u_x)/m \tag{16}$$

$$\ddot{y} = (u_4\ u_y)/m \tag{17}$$

$$\ddot{z} = (u_4 \cos\phi \cos\theta - mg)/m \tag{18}$$

In the mentioned set of equations from (13) to (18), the variables are $a_1 = (I_{yy} - I_{zz})/I_{xx}$, $b_1 = l/I_{xx}, c_1 = -J_r/I_{xx}, a_2 = (I_{zz} - I_{xx})/I_{yy}, b_2 = l/I_{yy}, c_2 = J_r/I_{yy}$, $a_3 = (I_{xx} - I_{yy})/I_{zz}$,

$b_3 = l/I_{zz}$ and $d_i = d_{si} + d_{ui}$, where the subscript $i = 1, 2, 3$. This term d_{si} shows the bounded disturbances, whereas the d_{ui} illustrates the unmodelled dynamic factors and external forces. In addition to this, one may note that the roll, pitch and yaw are the bounded input variables for our proposed underactuated quadrotor model. Thus, with bounded input and state variables, the derivative of input will also be bounded. This will lead towards the bounded change in the states as well and help in proving the stability of the proposed single-dimension fuzzy-based sliding mode control (SDF-SMC).

4. Control Design

This paper focuses on acquiring the accurate underactuated quadrotor dynamic model using model-free approach. To stabilize the system and reduce the tracking and position errors with minimum computation time and control input energy, a model-free single-dimension fuzzy-based sliding mode control (MFSDF-SMC) is proposed. This entire approach of MFSDF-SMC will ensure the greater accuracy of tracking with unknown and unmodelled dynamic factors.

4.1. Control Design Using Model-Free Approach

One may see a non-linear system as mentioned in [39,40], in implicit form:

$$f\big(y, \dot{y}, \ldots, u, \dot{u}, d\big) = 0 \tag{19}$$

Moreover, in this Equation (19), $y \in R$ is the output, $u \in R$ is the input variable and $d \in R$ is the bounded disturbances. Thus, the model-free control design is proposed here to approximate these dynamics of the system.

$$\ddot{y} = F(t) + \alpha u(t) \tag{20}$$

In above equation, $F(t)$ is defined as unknown expression that must be observed and estimated by checking the input and output relation. Then by deducing this for model-free control strategy, Equation (20) will be turned as:

$$\ddot{Y}_i = F_i(t) + \alpha_i u_i \tag{21}$$

For simplification, the notation in Equation (20) is indexed with i for the correspondence of individual inputs and state variables. The most important part of this strategy is the observing and estimating the unknown terms of F. Thus, the generalized form for proposed model-free control design is stated in Equation (20), where $\ddot{Y}_i$ is same as $\ddot{y}$ but illustrated as the sum of all corresponding individual inputs and state variables. Researchers have discussed this issue in several publications with different estimation techniques. This paper follows the estimation method followed by differentiator technique as mentioned in [40].

$$F(t) \approx \hat{F}(t) = F(t-\varepsilon) = \ddot{Y}(t-\varepsilon) - \alpha u(t-\varepsilon) \tag{22}$$

The term ε is defined as a small-time delay. Since the change in angular velocities and acceleration is bounded thus, this will lead $F(t)$ towards bounded values in Equation (22) and measurable using small delay and difference term as $F(t-\varepsilon)$. In this way, the model-free control can be stated as mentioned in Equation (23).

$$u_c = -\frac{\hat{F} - \ddot{Y}_d + u}{\alpha} \tag{23}$$

The term $\ddot{Y}_d$ is the required second derivative of the output state, and it should be smooth, whereas u_c is the feedback for measuring the tracking error. By manipulating Equations (22) and (23), one may get the relation as:

$$\ddot{e} + u_c = F - \hat{F} \tag{24}$$

where $\ddot{e}$ is defined as $Y - Y_d$, known as trajectory tracking error.

4.2. MFSDF-SMC Control Design Using Model-Free Approach

In this sub-section, we will develop single-dimension fuzzy-based sliding mode control, embed it with model-free approach, and discuss the conventional sliding mode control that has basic architecture consisting of steering infinite quadrotor's trajectory (in our case known as sliding manifold). Thus, it will lead the system to converge all the states towards zero asymptotically. The block diagram illustrates steering at provided helical trajectory in the Figure 1. For this research work and specifically for simulations, paper suggests the tracking of underactuated quadrotor over helical trajectory. The helical trajectory is among trajectories that exhibits real-world-like scenario [2]. In addition to this, it allows one to better evaluate and study the angular and translational parameters [3].

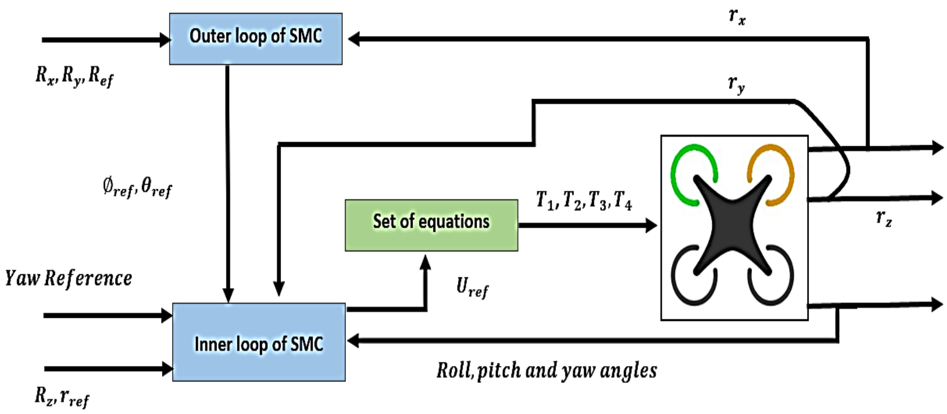

Figure 1. Conventional block diagram of SMC.

The above conventional SMC control technique is designed by following simple steps i.e., defining the sliding surface and later ensuring that all these variables move towards sliding surface. The next step is to develop the time delay estimation-based model-free SMC control as shown in Equation (27), which in Equation (25) is the tracking error and in (26) is the sliding surface:

$$e = Y - Y_d \tag{25}$$

whereas the sliding surface is defined as:

$$S = \dot{e} - ce \tag{26}$$

In Equation (26), variable c represents the gain of the proposed control scheme. Considering the Equation (23), the u_c can be given as:

$$u_c = -\frac{\hat{F} - \ddot{Y}_d + \dot{e} + ce}{\alpha} \tag{27}$$

where one may see

$$e_{est} = \ddot{e} + \dot{e} + ce \tag{28}$$

From Equation (26) or Equation (28), one can define $\dot{e}$,

$$\dot{S} = -\rho s - ksign(S) \tag{29}$$

In Equation (29), ρ and k are both positive diagonal definite matrices. After embedding the model-free approach with SMC, one may introduce the fuzzy logic control design. This is because of the stability requirement during aggressive maneuvers and avoidance of chattering noise (high number of oscillations on rotors) that may harm the propellers and BLDC motors too [53,65]. In this, the gains of SMC will be tuned by the fuzzy logic control (FLC), for which the main sliding surface and e and $\dot{e}$ will be computed as shown in Equations (29) and (30):

$$S = \begin{bmatrix} e & \dot{e} \end{bmatrix} \begin{bmatrix} k \\ 1 \end{bmatrix} \tag{30}$$

Moreover, the error and rate of change of error will be derived using the vectoral distance between state trajectory and manifold mathematically as shown in Equations (29) and (30) given as L_{sn} and L_o:

$$L_{sn} = \frac{(\dot{e_Q} + k\dot{e_Q})}{\sqrt{1+k^2}} \tag{31}$$

$$L_o = \sqrt{N^2 - {L_{sn}}^2} \tag{32}$$

This vectoral distance from point N to L_{sn} can be computed in this way, as illustrated in the Equations (31) and (32). Moreover, the pictorial illustration can be seen in Figure 2. In this conventional F-SMC technique, the set of rules are designed by considering L_{sn} and L_o as mainly an input to fuzzy logic controller, and the output of FLC is entertained as an input to SMC design to derive the states towards this sliding surface with appropriate time and with Zeno or chattering effect. Since the fuzzy logic design is based on linguistic variable scheme, the rules are also defined in the same manner as shown in Table 2 with triangular membership functions as illustrated on next page.

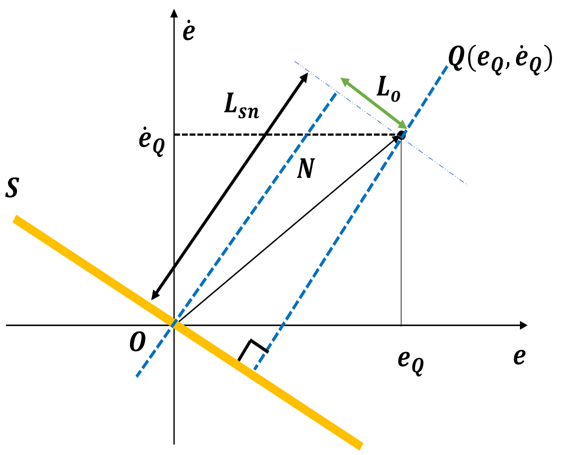

Figure 2. Vectoral distance between L_{sn} and L_o.

Table 2. Rule base for bounded-layer fuzzy-based SMC.

L_{sn} / L_o	NB	NS	NS	Z	PS	NS	PB
PB	Z	PS	PM	PB	PB	PB	PB
NS	NS	Z	PS	PM	PB	PB	PB
PS	NM	NS	Z	PS	PM	PB	PB
Z	NB	NM	NS	Z	PS	PM	PB
NS	NB	NB	NM	NS	Z	PS	PM
NS	NB	NB	NB	NM	NS	Z	PS
NB	NB	NB	NB	NB	NM	NS	Z

PB: Positive Big; NB: Negative Big; PM: Positive Medium; NM: Negative Medium; PS: Positive Small; NS: Negative Small; Z: Zero.

The Figure 2 is the graphical illustration for the variables L_{sn} and L_o on the basis of which the rule base for bounder-layer fuzzy-based SMC is computed. One may see these rules in Table 2 given below:

Furthermore, it is share that the output of this FLC design is based on singleton utilizing the concept of center of gravity (CoG) presented in the Figure 3. The entire range for all output and input membership functions as shown in Figures 3 and 4 respectively ranges in between −1 to 1, whereas the display ranges in between −0.6 and +0.6. The block diagram of this fuzzy-based sliding mode control is also shown in Figure 5.

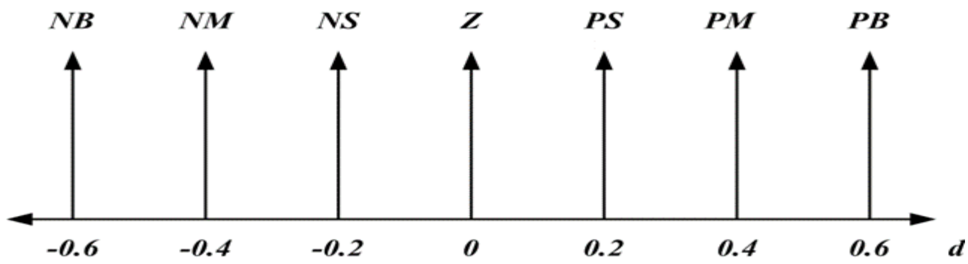

Figure 3. Output membership functions based on singleton (CoG).

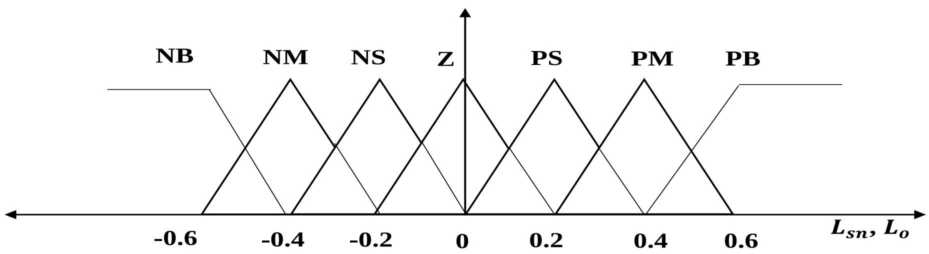

Figure 4. Input membership functions.

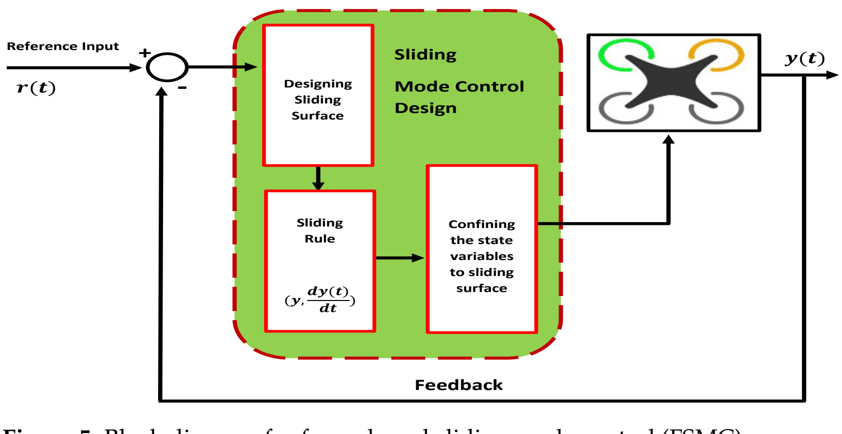

Figure 5. Block diagram for fuzzy-based sliding mode control (FSMC).

In this paper, two issues are discussed: the tackling of unmodelled dynamic factors using model-free approach and the suggestion of single-input- or dimension-based fuzzy sliding mode controller. It has been observed that fuzzy logic control design involves several steps: fuzzification, inference, and defuzzification. These individual steps consume some computation time that is computed and discussed in the results.

This computation time and control input energy derived using F-SMC control will not be suitable for aggressive maneuvers. Thus, paper recommends single input or dimension-based fuzzy sliding mode control. Single-dimension-based fuzzy sliding mode control (SDF-SMC) is designed using signed distance method [3,65] where one may convert the two-dimensional set of rules into single-dimension as shown in Table 3. This can only be done by taking another signed variable as "G" as illustrated in Figures 6 and 7 respectively. This signed variable "G" is a diagonal vector from previous table number 2.

$$L_{sn} + \alpha L_o = 0 \tag{33}$$

$$G = \frac{(L_{sn} + \alpha L_o)}{\sqrt{1+\alpha^2}} \tag{34}$$

Table 3. New table of rules based on single dimension.

G	GNB	GNM	GNS	GZ	GPS	GPM	GPS
G′	NB	NM	NS	Z	PS	PM	PB

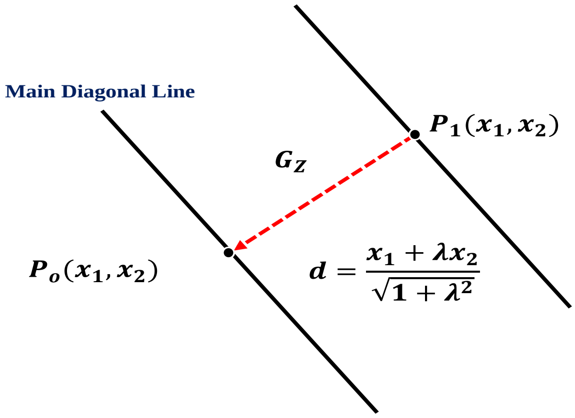

Figure 6. Graphical illustration for diagonal variable G.

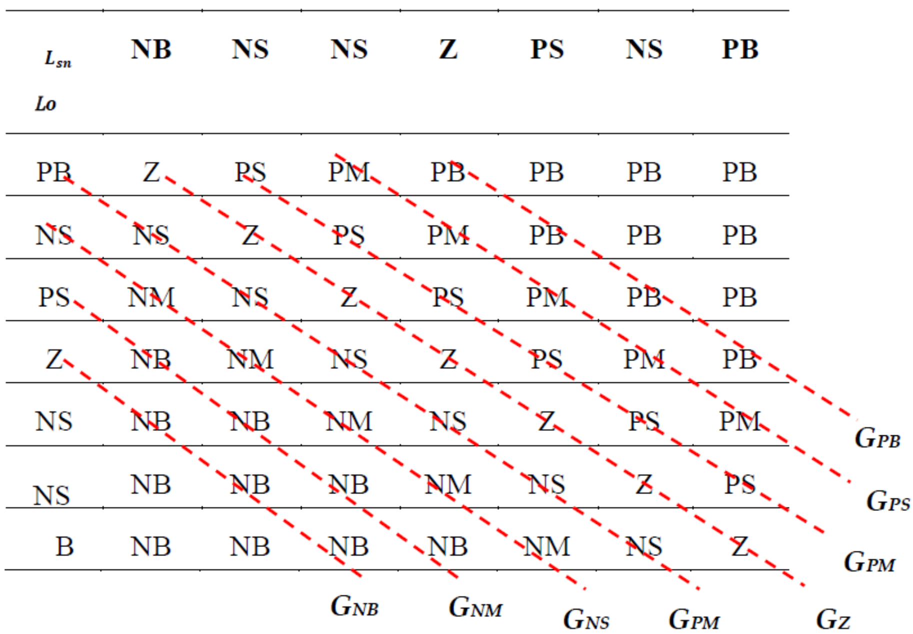

Figure 7. Using diagonals to derive the signed variable G.

As given in above figure, one may study this graphical illustration and may derive the relation. This is the method to convert the 2-D rule base table into single-dimension. The new rule base can be seen in Table 3. Whereas Figure 7 shows the pictorial demonstration for converting 2-dimensional table of rules into single dimension.

Moreover, the input functions are shown in Figure 8. The output function will be the same singleton based on center of gravity (CoG), along with the same block diagram as this is the only manipulation related to the fuzzy rules and the vectoral distance.

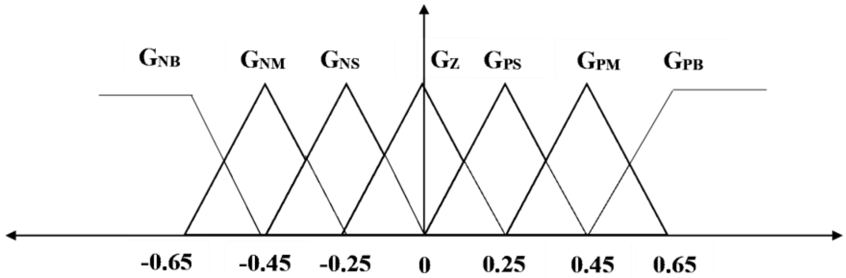

Figure 8. New revised input membership functions based on variable G.

4.3. Stability Analysis

In this sub-section, we have used the Lyapunov stability theorem, which is one of the classical methods used by several researchers to prove the stability of their proposed control designs. The Lyapunov function is given as:

$$V = V1 + V2 + V3 + \cdots \tag{35}$$

where each function can be illustrated in the form mentioned below as:

$$V_i = \frac{1}{2}z_i^2 + \frac{1}{\beta}\widetilde{c}_i^T + \widetilde{c}_i + \widetilde{\mathbf{p}}_i^T \mathbf{B}^{-1}{}_i\, \widetilde{\mathbf{p}}_i. \qquad for\ i = 1,2,3 \tag{36}$$

In the Equation (36), the variable z is given as $z = [z_1\ z_2\ z_3]^T$ and c is the varible that can be defined as $\widetilde{c} = \left[\widetilde{c}_1^T\ \widetilde{c}_2^T\ \widetilde{c}_3^T\right]$. Assume a bounded disturbance as $d(t)$. In this way, the time derivate will be:

$$\dot{V} = \sum_{i=1}^{3}(z_i\Big(\Lambda x_{i+3} + \Gamma_i(\mathbf{x})^T c_i + \epsilon_i + d_i + u_i\Big) - \widetilde{c}_i^T \dot{\hat{c}}_i \tag{37}$$

$$= \sum_{i=1}^{3}\Big(z_i\Big(\Lambda x_{i+3} + \Gamma_i(\mathbf{x})^T \hat{c}_i + \epsilon_i + d_i + u_i\Big) + \widetilde{c}_i^T\Big(\Gamma_i(\mathbf{x})z_i - \dot{\hat{c}}_i\Big)\Big) \tag{38}$$

Moreover, the control laws can be chosen as:

$$u_i = -\Lambda x_{i+3} - \Gamma_1^T \hat{c}_i - k_i z_i \tag{39}$$

$$\dot{\hat{c}}_i = \Gamma_1 z_i - v_i|z_i|\hat{c}_i \tag{40}$$

along with each k_i and v_i constant terms. There is a modification to update the bounded errors ϵ_i and the external disturbances d_i. This results in:

$$\dot{V}(z,\widetilde{c},t) = \sum_{i=1}^{3}(-k_i {z_i}^2 + z_i(\epsilon_i + d_i) - v_i|z_i|\widetilde{c}_i^T \dot{\hat{c}}_i \tag{41}$$

This will lead the $\dot{V}(z,\widetilde{c}) < 0$ from a compact set over the $(||z||,\ ||\widetilde{c}||)$ plane that includes the origin itself. Moreover, the smallest Lyapunov surface that encloses an invariant set such that it is a bound over the trajectories that start within the Lyapunov surface leads the signals to be uniformly bounded.

5. Simulation Results

To demonstrate effectiveness, this section illustrates the comparative analysis of conventional sliding mode control (SMC), fuzzy-based SMC and single-dimension fuzzy-based SMC design with and without model-free approach. All the simulation results are computed using MATLAB and Simulink software R2020a version. While executing the simple sliding mode control technique for underactuated quadrotor model, the drone deviates at 66.51 s and remains away from reference track till 70.51 s. One may see this impact of unmodelled dynamic factor during its maneuvering in Figure 9.

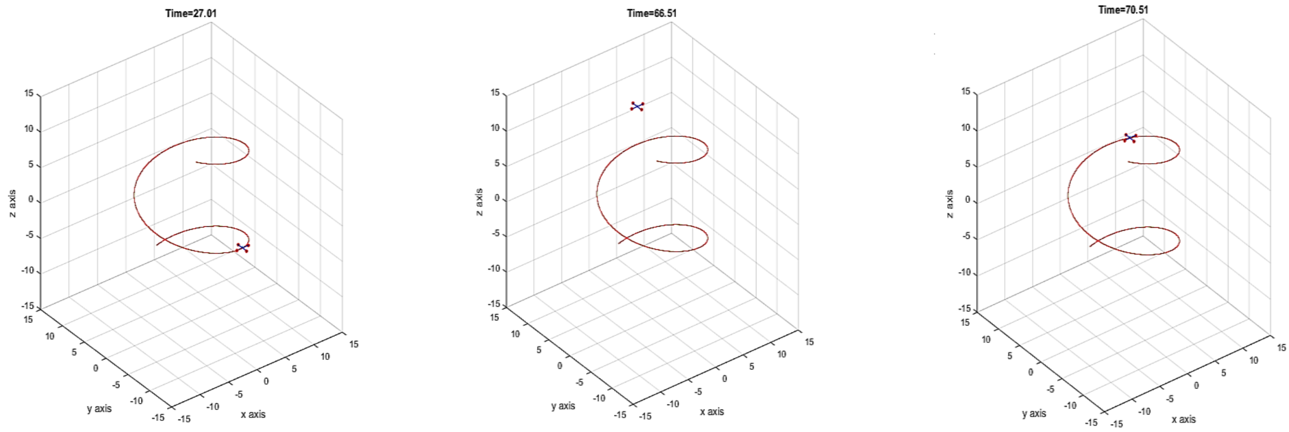

(**a**) (**b**) (**c**)

Figure 9. Quadrotor deviates from trajectory due to unmodelled dynamic factors.

In the results shown in Figure 10 are position trajectories on x, y and z axis. The unmodelled dynamic factors and unknown external disturbances are introduced in the simulation via a random function generator. One may see the underactuated quadrotor deviates at 25th second in all positional vectors. Moreover, the angular velocities such as roll, pitch and yaw responses are illustrated in Figure 11. This is the same with the angular velocities, where after introducing the unmodelled dynamic factors and external disturbance one may see the high number of oscillations at 25th second known as chattering or Zeno effect. This Zeno phenomenon is available in roll, pitch and even in yaw response.

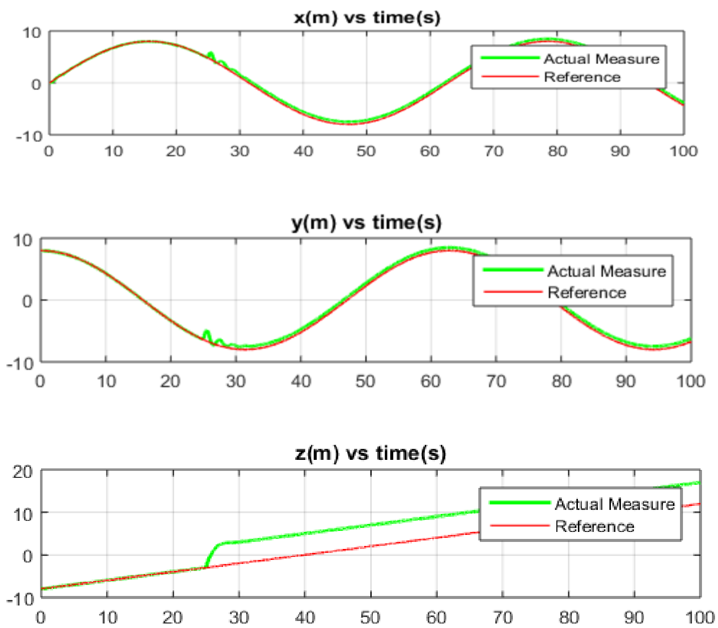

Figure 10. Position responses derived using SMC control technique.

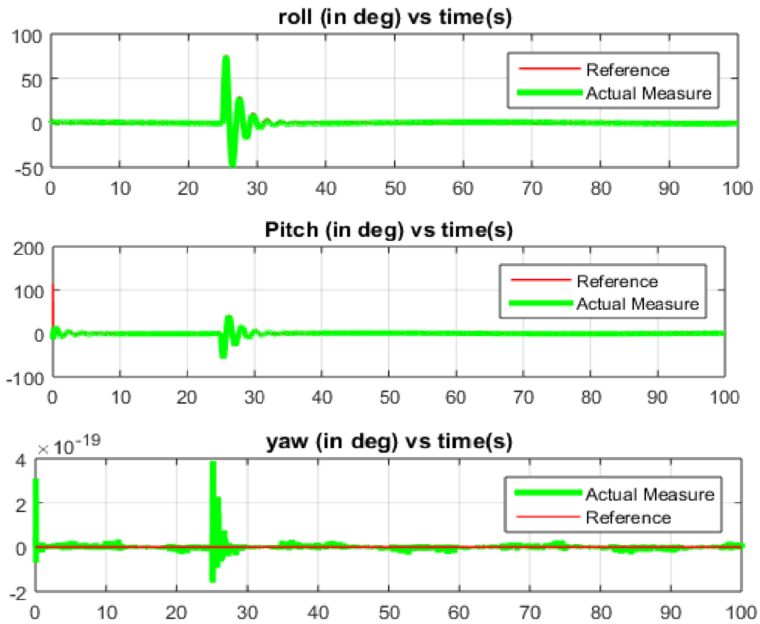

Figure 11. Roll, pitch and yaw responses using SMC Control technique.

Due to the high number of oscillations known as Zeno phenomenon, paper suggests the amalgamation of fuzzy logic design with sliding mode control. This constitutes a kind of underactuated quadrotor craft. The quadrotor deviates from the path at 59.51 s but again follows the same path at 63.51 s as one may remove the unmodelled dynamic factors and external disturbances. In addition to this, one may also see the chattering effect. Figure 12 shows the helical trajectory followed by quadrotor using conventional F-SMC control design, whereas Figure 13 shows the translational responses along with the angular velocities roll, pitch and yaw responses in Figure 14. This chattering effect is reduced once one amalgamates the fuzzy logic control design with sliding mode control.

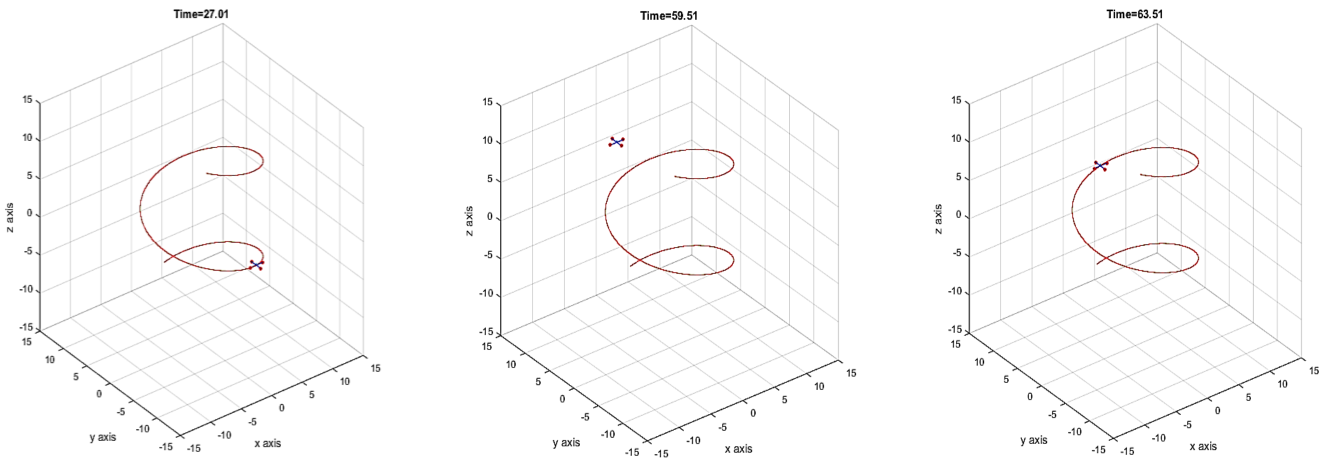

(**a**) (**b**) (**c**)

Figure 12. Quadrotor following helical trajectory using F-SMC control design.

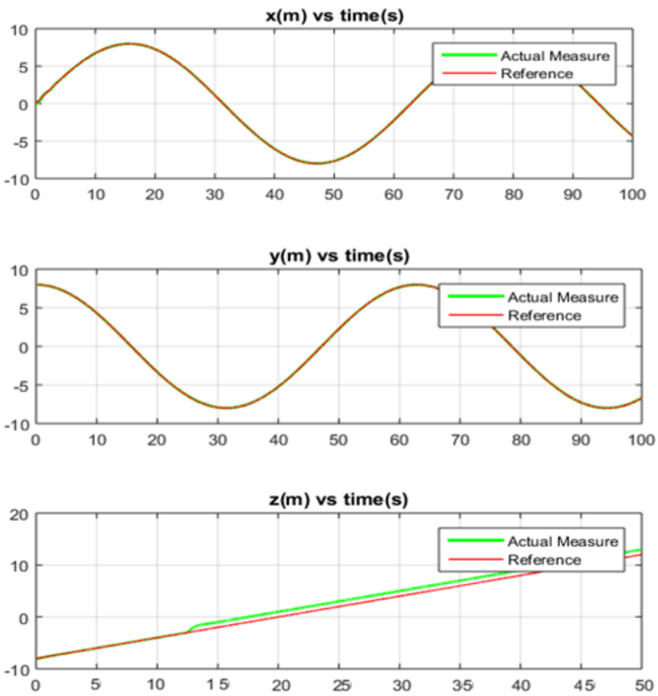

Figure 13. Position response derived using F-SMC control technique.

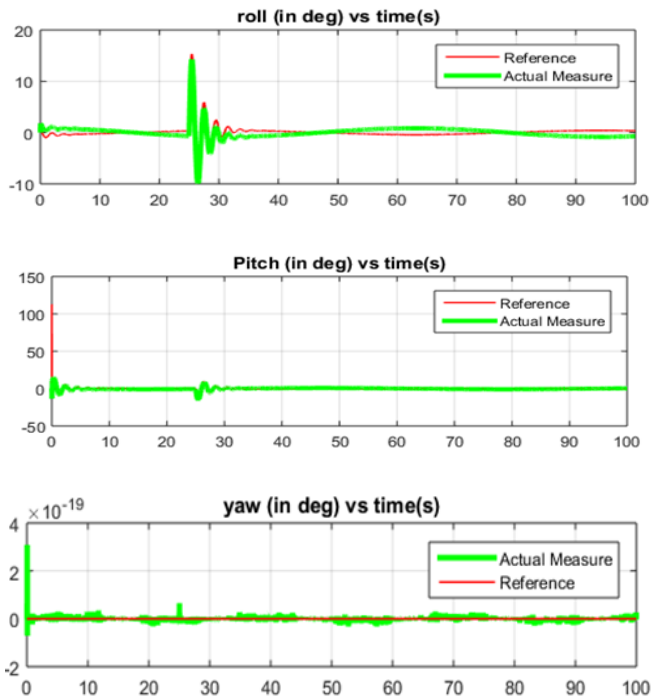

Figure 14. Roll, pitch and yaw response using F-SMC control technique.

The number of high oscillations is now reduced by using the conventional fuzzy-based sliding mode control (F-SMC). The graphs demonstrated in Figures 13 and 14 show that this technique can tackle the Zeno effect intelligently but cannot handle the unmodelled dynamic factors and external disturbances.

The only limitation of the SDF-SMC simulations as shown in Figures 15 and 16, is computation time that depends on fuzzification, inference of rules and defuzzification steps. This limits the underactuated quadrotor craft from doing aggressive maneuvers. The single-dimension-based fuzzy sliding mode control improves this response and enables the drone to perform aggressive maneuvers without chattering noise. Through the induction of unmodelled dynamic factors and external disturbance, same problem appears that our drone deviates from its track on 47.01 s and again comes on track at exactly 69.01 s, as demonstrated in Figure 17.

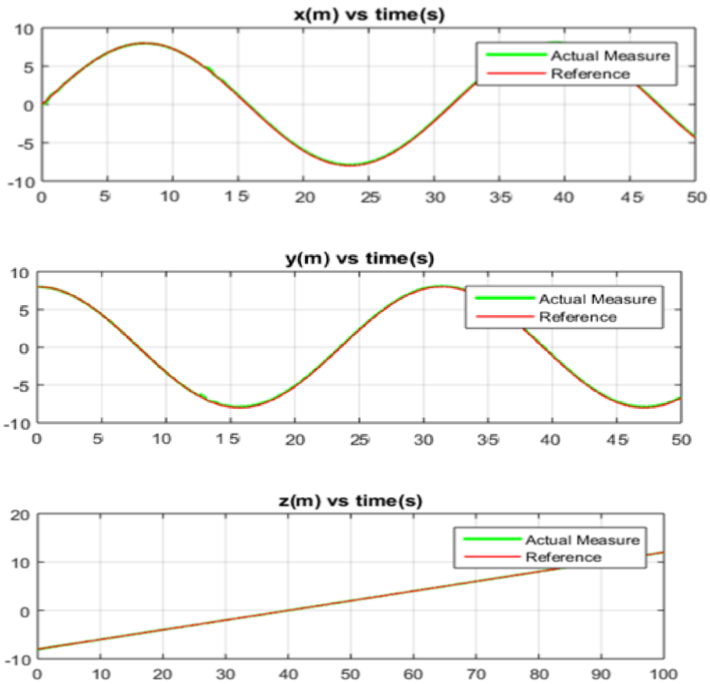

Figure 15. Position response derived using SDF-SMC control technique.

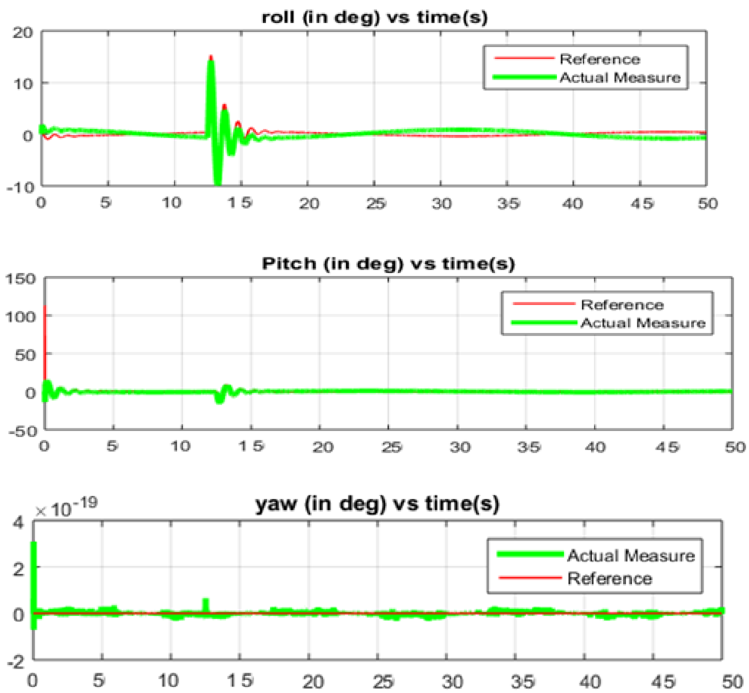

Figure 16. Roll, pitch and yaw responses using SDF-SMC control technique.

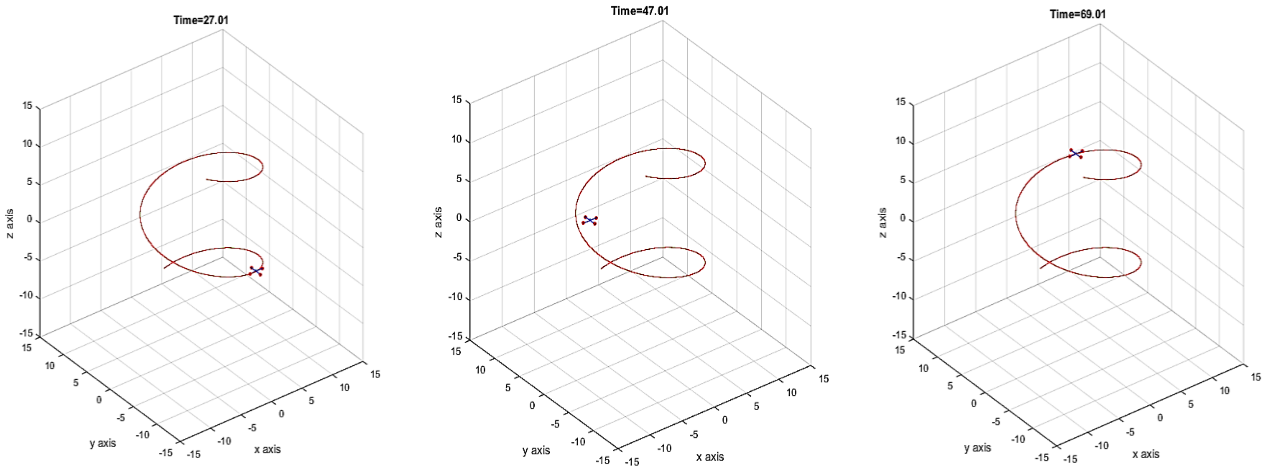

(**a**) (**b**) (**c**)

Figure 17. Quadrotor following helical trajectory using SDF-SMC (without model-free approach).

To tackle the unmodelled dynamic factors and external disturbances due to which underactuated quadrotor craft cannot follow the helical trajectory properly, paper proposes the model-free single-dimension fuzzy-based sliding mode control (MFSDF-SMC). The results of trajectory tracking are shown in Figure 18, whereas the translational and angular responses are shown in Figures 19 and 20, respectively.

Here, the underactuated quadrotor successfully improves its tracking performance and does not deviate from helical trajectory at any instant, but very low chattering effect is observed. The Table 4 compares and summarizes the entire performance of these techniques such as SMC, F-SMC, SDF-SMC and MFSDF-SMC control techniques. The comparison is done in terms of computational time, Zeno effect (chattering), control input energy and the duration for which it deviates from the track since SDF-SMC is 50% faster than the conventional F-SMC but deviates due to unmodelled dynamic factors and disturbances, whereas MFSDF-SMC algorithm improves the convergence time and tracking performance with no deviation from helical trajectory.

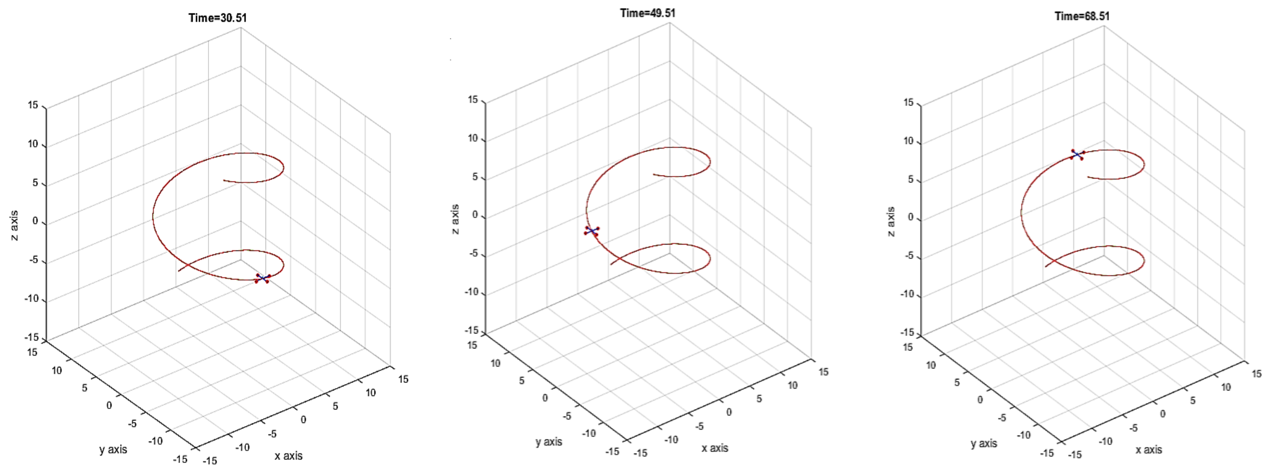

(**a**) (**b**) (**c**)

Figure 18. Quadrotor following helical trajectory using MFSDF-SMC control design.

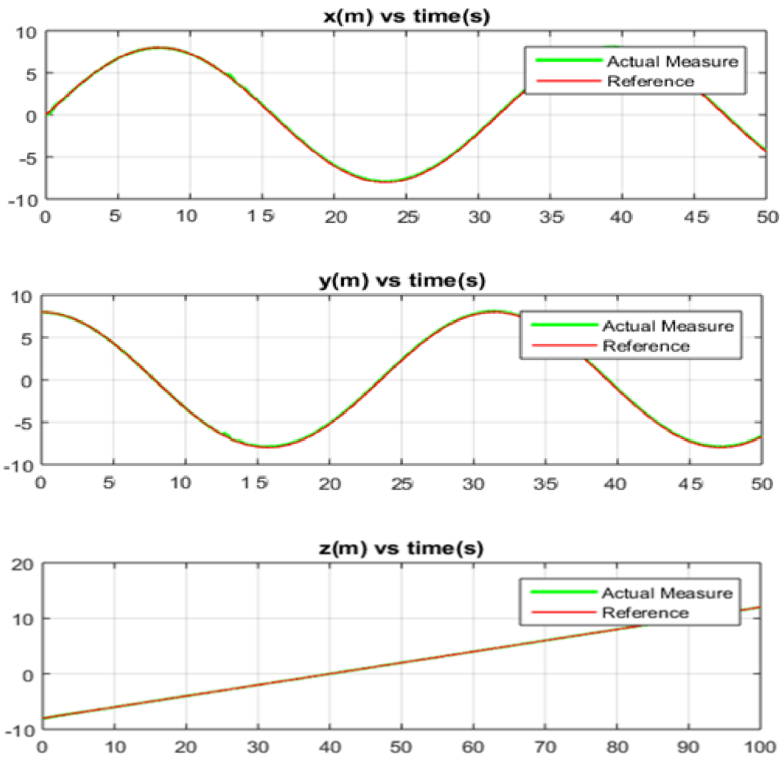

Figure 19. Position response derived using SDF-SMC control technique.

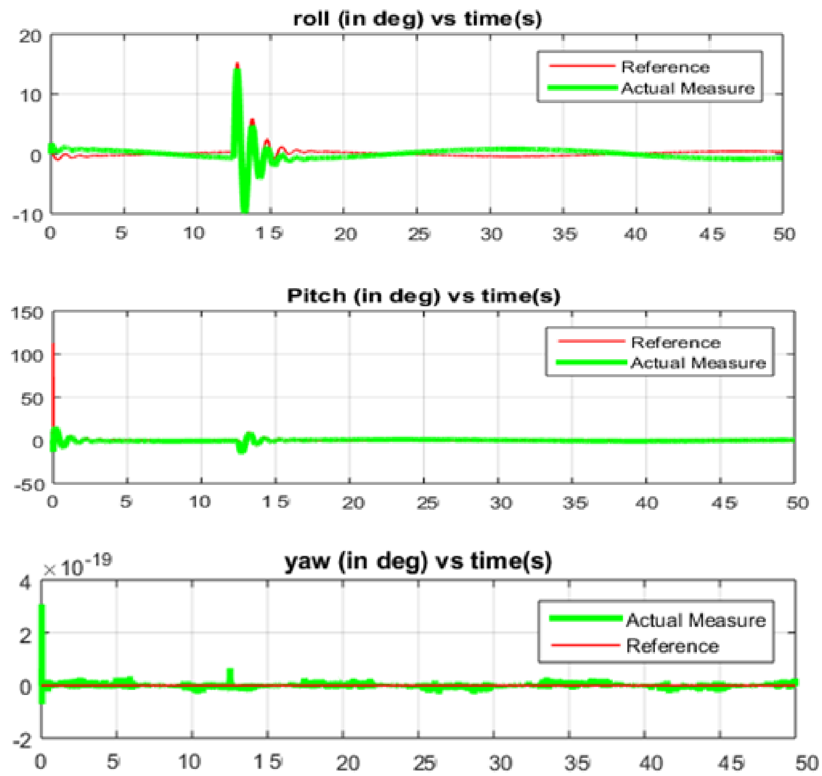

Figure 20. Roll, pitch and yaw responses using SDF-SMC control technique.

Table 4. Comparison between SMC, F-SMC, SDF-SMC and MFSDF-SMC algorithms.

Control Designs	Execution Time (s)	Chattering Effect	Control Input Energy (CIE)	Deviation Time (s)
SMC	100	4.25%	5.54%	4.0
F-SMC	100	3.25%	5.54%	4.0
SDF-SMC	50	2.35%	3.75%	22
MFSDF-SMC	50	2.03%	3.07%	0

Table 4 improves the factors commented on in [3]. In addition to these factors, the execution time is also improved; this is the total simulation time taken for the entire scenario under the availability of unmodelled dynamic factors. For readers, the error rates for proposed model-free single-dimension fuzzy-based sliding mode control are shown in Figures 21 and 22.

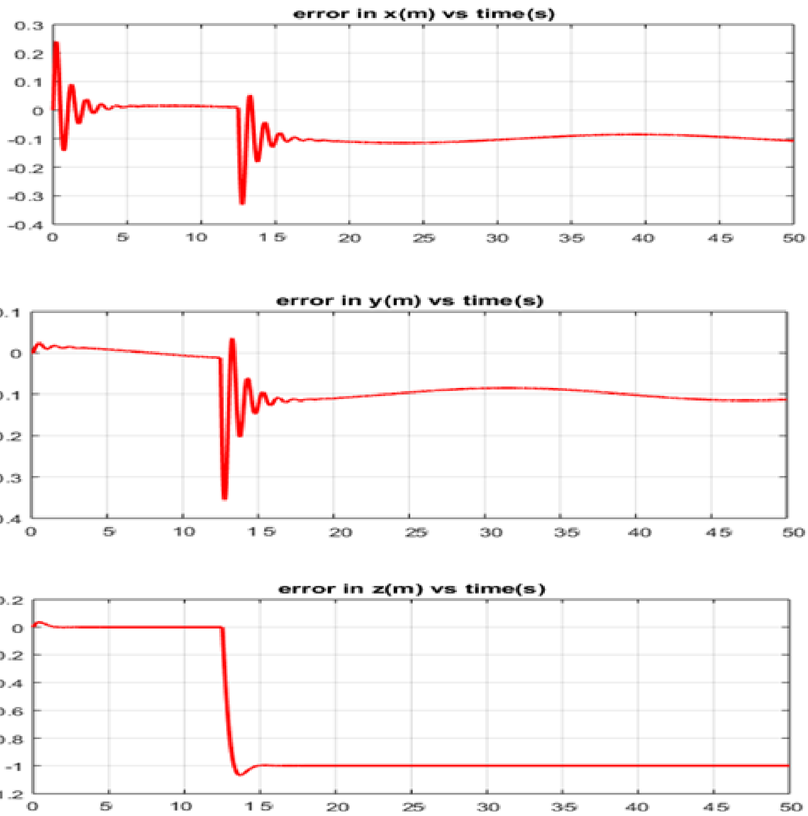

Figure 21. Position error rates while maneuvering using MFSDF-SMC.

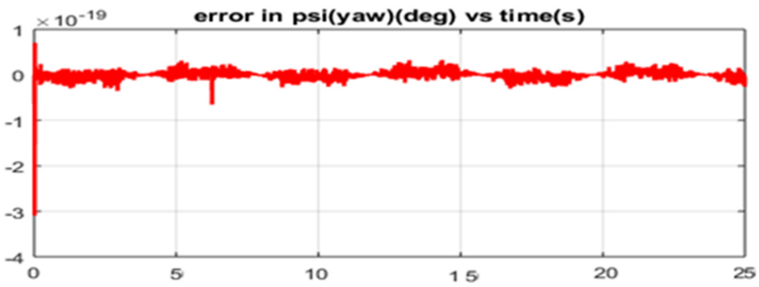

Figure 22. Yaw error rates while maneuvering using MFSDF-SMC.

The total control input energy (CIE) as mentioned in Table 4 is the total power consumption by the four rotors of quadrotor. It is calculated using ordinary integral square method. The same method is used for the computation of chattering phenomena. The integral square error can be utilized mathematically as given below:

$$ISE = \int_0^\infty e^2(t)\, dt \tag{42}$$

In Equation (42), e is defined as an error generated via the difference between the two oscillations. Table 5 shows the improvement acquired after the implementation of our proposed MFSDF-SMC algorithm.

Table 5. Performance summary between SMC, F-SMC, SDF-SMC and MFSDF-SMC.

Control Designs	Chattering Effect	Delay in Accelerations	Estimation Delay	Steady-State Error	Overshoots 10–15%	Settling Time
SMC	Yes	Yes	Yes	4.0	Yes	Huge
F-SMC	Yes	Yes	Yes	4.0	Yes	Huge
SDF-SMC	Yes	Yes	Yes	22	Yes	Huge
MFSDF-SMC	No	No	Yes	0	Reduced	Small

In the Table 5, one may see the factors have been improved by the implementation of model-free single-dimension fuzzy-based sliding mode control design. The only limitation of this algorithm is the estimation of the states as one may see some time delay while estimating the states.

As far as transient and steady-state issues are considered, one may see that steady-state error in percentage is 4% in SMC and FSMC, while it dramatically increased for SDF-SMC. Similarly with overshoots, maximum the overshoot generated through SMC, F-SMC and SDF-SMC is in between 10 and 15%. If one may see the settling time, it seems quadrotor has sluggishness in tracking the trajectory. The entire results are computed by running the simple command in MATLAB for the state space model, i.e., step (A B C D), where A, B, C and D are the state space matrices for the underactuated quadrotor craft. From this entire Table 5, the MFSDF-SMC seems effective and robust.

6. Hardware Configuration and Experiment

The paper suggests the specific configuration for our designed underactuated quadrotor craft that is demonstrated in Figure 23.

The quadrotor type proposed in this hardware configuration is completely customized and may carry variable payload from dull, difficult, and dirty situations. The prototype used in this paper is RC eye 650 proposed by RC Logger that can easily be purchased from Heli distributors. The proposed RC eye 650 consists of 6 degrees of freedom with only four Brushless DC (BLDC) motors. The four BLDC motors are distributed at same distance from the center of mass. There is a tank attached to it with some liquid. The idea behind attaching this tank is to utilize this drone for spraying disinfectants initially and secondly to check the case of smooth and non-smooth payload variation.

The proposed underactuated unmanned aerial vehicle can spray the disinfectants from one place to another. Moreover, this difficult task can be performed easily due to use of pigeon eye view via zenmuse HD gimbal-based camera. The drone carries the additional battery so that the flight time can be extended up to 50 min more to spray approximately 3-L disinfectant solution. The underactuated quadrotor craft used in this prototype consists of the following mentioned components.

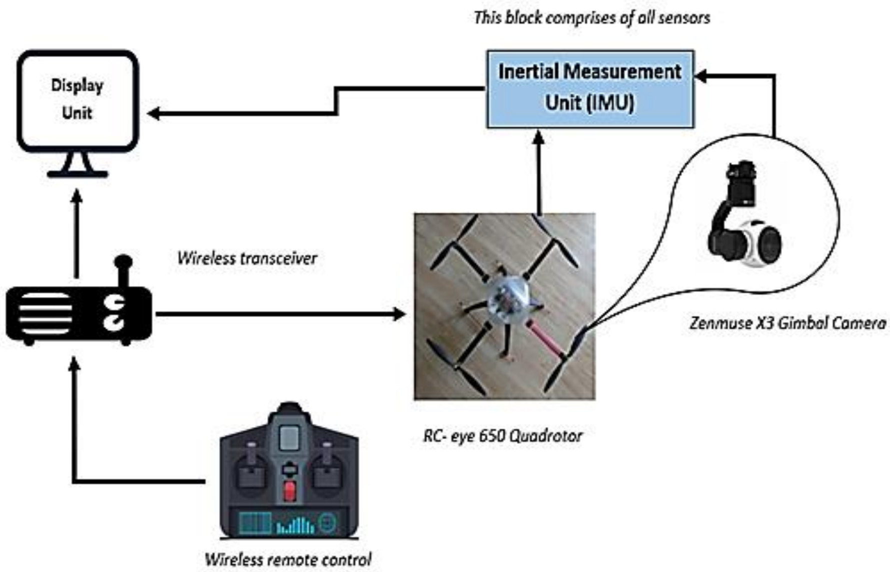

Figure 23. Block diagram demonstrating the experimental setup.

6.1. PIXHAWK PX4 Flight Controller

The main component in this entire hardware setup known as brain of this under-actuated quadrotor is the controller. The proposed controller in this hardware design is PIXHAWK PX4 version of flight controller. This will deal with all types of maneuvering operations. This controller has better capability to tackle the control of all BLDC motors, power distribution, radio transmission and above all the global positioning satellite (GPS). This is the controller with 32-bit microprocessor, 256 KB random access memory and 2 MB flash memory, along with gyroscopic sensor, barometer and 14-bit magnetometer, which make it a one of a kind and most suitable for our experiment. In addition to these features, it has 14 pulse width modulation (PWM) output channels along with autopilot facility and GPS.

6.2. Wireless Remote Control (WRC)

The RC-eye 650 is dully controlled through wireless remote control (WRC) that has the range of 2.400 to 2.5 GHz. In addition to this, this has been integrated with special Lightbridge controller module to make it flexible so that one can control it using cellular device too. The range in terms of distance through which one may transmit the control inputs is in between 1.65 to 4.55 km with receiver's sensitivity of −101 dBm (+) (−) 2 dBm. Moreover, the temperature range at which one may operate it is −10 to 45 degrees Celsius. This wireless control technique supports android as well as iPhone operating systems. The name of application is DJI app. The mentioned controller in this manuscript supports the high-definition (HD) camera view using zenmuse X3 gimbal camera, as illustrated in the Figure 23.

6.3. Propulsion System

The propulsion system is one of the forms of DJI E800 series electrical version. This will energize our underactuated quadrotor and enable it to have a stable flight. There are four electronic speed controllers popularly known as (ESC) that help us to vary the speed of four propellers followed by BLDC motors.

6.4. Global Positioning System (GPS)

Our RC eye 650 is mainly embedded with GPS-based tracking system, which will help us in real time to track our underactuated quadrotor; in addition to this, it supports the faster satellite communication. This also has guidance system that works using optical and ultrasonic sensors embedded within the inertial measurement unit (IMU) as highlighted in the Figure 19. The RC-eye 650 quadrotor is then operated under the influence of variable wind disturbance and variable payload conditions with the model-free single-dimension-based fuzzy sliding mode control. The acquired position errors are shown in the Figure 24. These errors are same as shown in the Figure 21. This validates the proposed algorithm.

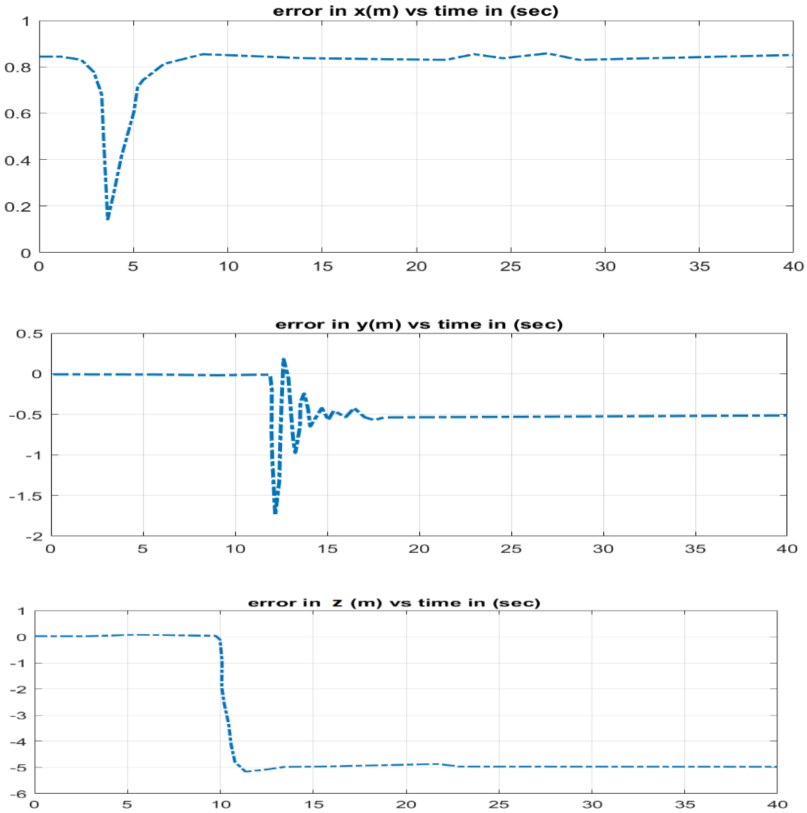

Figure 24. Position error rates while maneuvering using MFSDF-SMC during hardware implementation.

6.5. Error Rates and Flight Mode of Underactuated Quadrotor

The Figure 24 shows the performance of proposed control algorithm when implemented in practical scenario. One may see the underactuated quadrotor while maneuvering produces the same position error rates as expected in a closed environment. The most prominent guidance is involved here by using GPS module. This is because this module further comprises of several core processing units and sensors such as optical-odometer, 3D sensing and obstacle sensing images. Every unit facilitates in tracking the helical trajectory so that optical odometer performs the measurements related to the speed of the proposed underactuated quadrotor, and 3D sensing helps in sensing the three-dimensional space. Obstacles are also tackled properly along with precise vision-based positioning system.

There is a minor time delay while executing the control inputs after the execution of experimental setup in open environment only. This can be improved using Pade approximation method and opting for better wireless remote controller but is not needed in closed environment, as demonstrated in this paper. It should be noted that the experiment was performed in a closed jurisdiction by keeping the same conditions within the project lab. The flight performed by quadrotor was the same helical path within the closed jurisdiction, as shown in the Figure 25.

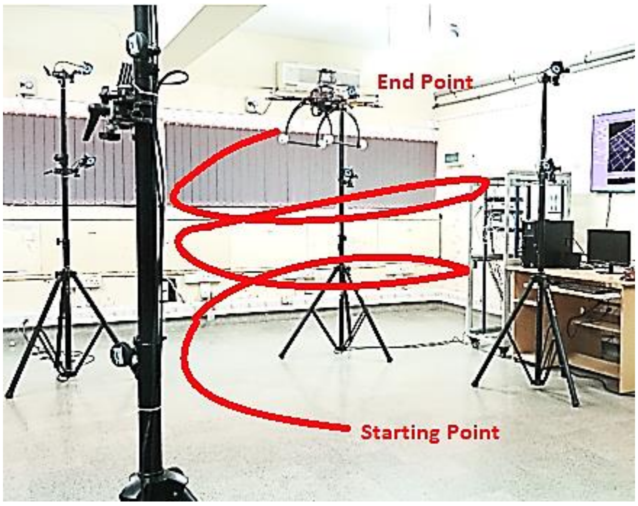

Figure 25. Flight mode of quadrotor within a closed environment.

7. Conclusions

The proposed system in this manuscript is a quadrotor unmanned aerial vehicle. This is known as one of the most underactuated systems because it has a smaller number of control inputs than degrees of freedom (DOF). This is a major issue that is very hard to control and stabilize. This manuscript shows a comparative performance analysis between sliding mode control (SMC), conventional fuzzy-based sliding mode control (FSMC) and single-dimension-based fuzzy sliding mode control without a model-free approach (SDF-SMC) and with a model-free approach (MFSDF-SMC).

First, the paper addresses that the sliding mode control (SMC) algorithm is highly sensitive to external disturbances and unmodelled dynamic factors. Thus, by implementing this SMC design one may see that the four brushless DC (BLDC) motors of the quadrotor craft are experiencing a high number of oscillations known as Zeno phenomenon or chattering noise. The main reason for this noise is the design of manifold or sliding surface design for SMC algorithm.

Secondly, to have a smooth sliding surface, the paper discusses the amalgamation of fuzzy logic control with SMC design, but this increases the execution time as well as the control input energy (CIE). This results in slow convergence of all error rates as well as sluggish maneuvers of quadrotor because of further sub-steps involved in FSMC algorithm such as fuzzification, inference of rules and defuzzification. In addition to this, both SMC and fuzzy-based SMC algorithms cannot enable the drone to follow the helical trajectory properly and generate some transient as well as steady-state issues. One may see the Zeno effect in both algorithms.

Thirdly, the paper suggests the single-dimension fuzzy sliding mode control (SDF-SMC) design to tackle the unmodelled dynamic factors and deal with the high number of oscillations known as the Zeno phenomenon or the chattering effect. One can see the employment of a mathematical approach named as single-dimension method to turn the two-dimensional rules into a single dimension. In this technique, there is still noticeable diversion while tracking the helical trajectory in the presence of unmodelled dynamic factors but comparatively better transient and steady-state performance than SMC and conventional FSMC algorithms.

Finally, the model-free approach is merged with single-dimension fuzzy-based sliding mode control (MFSDF-SMC). The simulation results in comparison with SMC, FSMC and SDF-SMC without model-free approach have been demonstrated. These results prove the robustness of the proposed algorithm for the stability and control of an underactuated quadrotor UAV under aggressive maneuvers and for tracking the helical trajectory in the presence of unmodelled dynamic factors and external disturbances.

8. Future Work and Recommendation

In this paper, the model-free single-dimension fuzzy sliding mode control design seeks to address issues such as gimbal lock, unmodelled dynamic factors, computation time, chattering effect, control input energy and some transient and steady-state errors. Future work is now focused on extensive nonlinear extended-state observations and disturbance observations with this same approach to reduce the estimation delays, and mathematical approaches such as the pade approximation method to reduce the time delay in accelerations to improve maneuverability in the presence of unmodelled dynamic factors and external disturbances. In addition to this, some of the quantitative analysis work will also be dedicated to evaluating the error rates while executing more experimental work.

Author Contributions: Conceptualization, G.E.M.A. and V.S.A.; methodology, G.E.M.A.; software, G.E.M.A.; Z.A.A. validation, S.A.B.M.Z. and V.S.A.; formal analysis, Z.A.A.; and V.S.A. investigation, G.E.M.A.; resources, S.A.B.M.Z.; writing—original draft preparation, G.E.M.A.; writing—review and editing, S.A.B.M.Z.; and V.S.A. visualization, Z.A.A.; supervision, S.A.B.M.Z.; project administration, V.S.A.; funding acquisition, S.A.B.M.Z. and Z.A.A. All authors have read and agreed to the published version of the manuscript.

Funding: This research was funded by Yayasan Universiti Teknologi PETRONAS (YUTP), grant number 015LC0-316, and the APC was funded by Research Management Centre, Universiti Teknologi PETRONAS, Malaysia under the same grant.

Data Availability Statement: The study did not report any data.

Acknowledgments: The author wishes to extend his sincere thanks to the Center of Graduate Studies, Universiti Teknologi, PETRONAS, Malaysia for providing state-of-the-art research facilities to carry out this work. He is also grateful to them for providing an opportunity to work in a Graduate Research Assistantship Scheme to pursue his doctoral studies at the Department of Electrical and Electronic Engineering under Yayasan Universiti Teknologi PETRONAS (YUTP) Funding, grant number 015CL0-316. In addition, the author is thankful for the support provided under the Startup grant funded by School of Systems Science, Beijing Normal University, Zhuhai, China to carry out experimental work.

Conflicts of Interest: The authors declare no conflict of interest.

References

1. Abro, G.E.M.; Asirvadam, V.S.; Zulkifli, S.A.B.; Raza, S.A. Review of Hy-brid Control Designs for Underactuated Quadrotor with Unmodelled Dynamic Factors. In Proceedings of the International Conference for Emerging Technologies in Computing, London, UK, 19–20 August 2020; Springer: Berlin/Heidelberg, Germany, 2020; pp. 62–85.
2. Li, Y.; Song, S. A survey of control algorithms for Quadrotor Unmanned Helicopter. In Proceedings of the 2012 IEEE Fifth International Conference on Advanced Computational Intelligence (ICACI), Nanjing, China, 18–20 October 2012; pp. 365–369.
3. Abro, G.E.M.; Asirvadam, V.S.; Zulkifli, S.A.B.M.; Sattar, A.; Kumar, D.; Anwer, A. Effects of unmodelled dynamic factors on an under-actuated quadrotor: A review of hybrid observer design methods. *Meas. Control* **2020**, *53*, 1978–1987. [CrossRef]
4. Sangyam, T.; Laohapiengsak, P.; Chongcharoen, W.; Nilkhamhang, I. Path tracking of UAV using self-tuning PID controller based on fuzzy logic. In Proceedings of the SICE Annual Conference 2010, Taipei, Taiwan, 18–21 August 2010; IEEE: Piscataway, NJ, USA, 2010; pp. 1265–1269.
5. Ali, Z.A.; Jabeen, B. Prototyping Non-holonomic Hovercraft for Path Planning and Obstacle Avoidance. *Sir Syed Univ. Res. J. Eng. Technol.* **2019**, *9*, 7–12.
6. Khalid, A. Performance Analysis of Mars Powered Descent based Landing in Constrained Optimization Control Framework. Ph.D. Thesis, Department of Electrical Engineering, COMSATS University Islamabad, Islamabad, Pakistan, 2019.
7. Panomrattanarug, B.; Higuchi, K.; Mora-Camino, F. Attitude control of a quadrotor aircraft using LQR state feedback controller with full order state observer. In Proceedings of the The SICE Annual Conference 2013, Nagoya, Japan, 14–17 September 2013; IEEE: Piscataway, NJ, USA, 2013; pp. 2041–2046.
8. Zhang, Y.-D.; Wu, L.; Wang, S. UCAV Path Planning by Fitness-Scaling Adaptive Chaotic Particle Swarm Optimization. *Math. Probl. Eng.* **2013**, *2013*, 1–9. [CrossRef]
9. Dydek, Z.T.; Annaswamy, A.M.; Lavretsky, E. Adaptive Control of Quadrotor UAVs: A Design Trade Study with Flight Evaluations. *IEEE Trans. Control Syst. Technol.* **2012**, *21*, 1400–1406. [CrossRef]
10. Bergamasco, M.; Lovera, M. Identification of Linear Models for the Dynamics of a Hovering Quadrotor. *IEEE Trans. Control Syst. Technol.* **2014**, *22*, 1696–1707. [CrossRef]

11. Ryan, T.; Kim, H.J. LMI-Based Gain Synthesis for Simple Robust Quadrotor Control. *IEEE Trans. Autom. Sci. Eng.* **2013**, *10*, 1173–1178. [CrossRef]
12. Bouabdallah, S.; Siegwart, R. Backstepping and sliding-mode techniques applied to an indoor micro quadrotor. In Proceedings of the 2005 IEEE International Conference on Robotics and Automation, Barcelona, Spain, 18–22 April 2005; IEEE: Piscataway, NJ, USA, 2005; pp. 2247–2252.
13. Dierks, T.; Jagannathan, S. Output Feedback Control of a Quadrotor UAV Using Neural Networks. *IEEE Trans. Neural Netw.* **2010**, *21*, 50–66. [CrossRef]
14. Mahony, R.; Kumar, V.; Corke, P. Multirotor Aerial Vehicles: Modeling, Estimation, and Control of Quadrotor. *IEEE Robot. Autom. Mag.* **2012**, *19*, 20–32. [CrossRef]
15. Mokhtari, M.R.; Cherki, B. Robust control for attitude tracking problem for a quadrotor unmanned aerial vehicle. In Proceedings of the 3rd International Conference on Systems and Control, Algiers, Algeria, 29–31 October 2013; IEEE: Piscataway, NJ, USA, 2013; pp. 862–867.
16. Lee, T. Robust Adaptive Attitude Tracking on SO(3) With an Application to a Quadrotor UAV. *IEEE Trans. Control Syst. Technol.* **2013**, *21*, 1924–1930. [CrossRef]
17. Grzonka, S.; Grisetti, G.; Burgard, W. A Fully Autonomous Indoor Quadrotor. *IEEE Trans. Robot.* **2011**, *28*, 90–100. [CrossRef]
18. Cabecinhas, D.; Naldi, R.; Marconi, L.; Silvestre, C.; Cunha, R. Robust Take-Off for a Quadrotor Vehicle. *IEEE Trans. Robot.* **2012**, *28*, 734–742. [CrossRef]
19. Liu, H.; Bai, Y.; Lu, G.; Zhong, Y. Robust attitude control of uncertain quadrotors. *IET Control Theory Appl.* **2013**, *7*, 1583–1589. [CrossRef]
20. Ullah, S.; Mehmood, A.; Khan, Q.; Rehman, S.; Iqbal, J. Robust Integral Sliding Mode Control Design for Stability Enhancement of Under-actuated Quadcopter. *Int. J. Control Autom. Syst.* **2020**, *18*, 1671–1678. [CrossRef]
21. Wasim, M.A.; Ullah, M.; Iqbal, J.A. Gain-scheduled proportional integral derivative control of taxi model of unmanned aerial vehicles. *Rev. Roum. Sci. Tech. Ser. Electrotech. Energ.* **2019**, *64*, 75–80.
22. Ajwad, S.A.; Iqbal, J.; Islam, R.U.; Alsheikhy, A.; Almeshal, A.; Mehmood, A. Optimal and Robust Control of Multi DOF Robotic Manipulator: Design and Hardware Realization. *Cybern. Syst.* **2018**, *49*, 77–93. [CrossRef]
23. Qi, W.; Zong, G.; Karimi, H.R. Sliding Mode Control for Nonlinear Stochastic Singular Semi-Markov Jump Systems. *IEEE Trans. Autom. Control* **2020**, *65*, 361–368. [CrossRef]
24. Qi, W.; Zong, G.; Karim, H.R. Observer-based adaptive SMC for nonlinear uncertain singular semi-Markov jump systems with applications to DC motor. *IEEE Trans. Circuits Syst. I Regul. Pap.* **2018**, *65*, 2951–2960. [CrossRef]
25. Chen, K.; Shi, Z.; Tong, S.; Dong, Y.; Chen, J. Aerodynamic interference test of quad tilt rotor aircraft in wind tunnel. *Proc. Inst. Mech. Eng. Part G J. Aerosp. Eng.* **2019**, *233*, 5553–5566. [CrossRef]
26. Mo, H.; Farid, G. Nonlinear and Adaptive Intelligent Control Techniques for Quadrotor UAV—A Survey. *Asian J. Control* **2019**, *21*, 989–1008. [CrossRef]
27. Benosman, M.; Lewis, F.L.; Guay, M.; Owens, D. Editorial for the Special Issue on Learning-based Adaptive Control: Theory and Applications. *Int. J. Adapt. Control Signal Process.* **2019**, *33*, 225–227. [CrossRef]
28. Vahdanipour, M.; Khodabandeh, M. Adaptive fractional order sliding mode control for a quadrotor with a varying load. *Aerosp. Sci. Technol.* **2019**, *86*, 737–747. [CrossRef]
29. Jasim, O.A.; Veres, S.M. A robust controller for multi rotor UAVs. *Aerosp. Sci. Technol.* **2020**, *105*, 106010. [CrossRef]
30. Wang, J.; Bierling, T.; Achtelik, M.; Hocht, L.; Holzapfel, F.; Zhao, W.; Go, T. Attitude Free Position Control of a Quadcopter using Dynamic Inversion. In *Infotech@Aerospace 2011*; American Institute of Aeronautics and Astronautics: Reston, VA, USA, 2011; p. 1583.
31. Wang, X.; Sun, S.; Van Kampen, E.-J.; Chu, Q. Quadrotor Fault Tolerant Incremental Sliding Mode Control driven by Sliding Mode Disturbance Observers. *Aerosp. Sci. Technol.* **2019**, *87*, 417–430. [CrossRef]
32. Spong, M.W.; Hutchinson, S.; Vidyasagar, M. *Robot Modeling and Control*; John Wiley & Sons: Hoboken, NJ, USA, 2020.
33. Sciavicco, L.; Bruno, S. *Modelling and Control of Robot Manipulators*; Springer Science & Business Media: Berlin, Germany, 2012.
34. Wang, H.; Chi, Z.; Tianwei, S.; Fuwang, W.; Shujun, M. Real-time EEG-based detection of fatigue driving danger for accident prediction. *Int. J. Neural Syst.* **2015**, *25*, 1550002. [CrossRef] [PubMed]
35. Tian, Y.; Wang, H.; Vasseur, C. Adaptive optimal trajectory tracking control of nonlinear affine in control system with unknown internal dynamics. In Proceedings of the 33rd Chinese Control Conference, Nanjing, China, 28–30 July 2014; pp. 2234–2239.
36. Wang, H.; Vasseur, C.; Christov, N.; Koncar, V. Vision servoing of robot systems using piecewise continuous controllers and observers. *Mech. Syst. Signal Process.* **2012**, *33*, 132–141. [CrossRef]
37. Youcef-Toumi, K.; Fuhlbrigge, T.A. Application of decentralized timedelay controller to robot manipulators. In Proceedings of the 1989 IEEE International Conference on Robotics and Automation, Scottsdale, AZ, USA, 14–19 May 1989; pp. 1786–1787.
38. Fliess, M.; Join, C. Model-free control. *Int. J. Control* **2013**, *86*, 2228–2252. [CrossRef]
39. Fliess, M.; Join, C. Stability Margins and Model-Free Control: A First Look. In Proceedings of the 2014 European Control Conference (ECC), Strasbourg, France, 24–27 June 2014; pp. 454–459.
40. Al Younes, Y.; Drak, A.; Noura, H.; Rabhi, A.; El Hajjaji, A. Model-Free Control of a Quadrotor Vehicle. In Proceedings of the 2014 International Conference on Unmanned Aircraft Systems (ICUAS), Orlando, FL, USA, 27–30 May 2014; pp. 1126–1131.

41. Ishaque, K.; Abdullah, S.S.; Ayob, S.; Salam, Z. A simplified approach to design fuzzy logic controller for an underwater vehicle. *Ocean Eng.* **2011**, *38*, 271–284. [CrossRef]
42. Ahmad, M.A.; Saealal, M.S.; Ismail, R.M.T.R.; Zawawi, M.A.; Nasir, A.N.K.; Ramli, M.S.; Barsoum, N.; Webb, J.F.; Vasant, P. SIngle Input Fuzzy Controller with Command Shaping Schemes for Double-Pendulum-Type Overhead Crane. *AIP Conf. Proc.* **2011**, *1337*, 113–117. [CrossRef]
43. Tiwari, K.N.; Waghmare, L.M.; Krishnankutty, P. Single Input Fuzzy Logic Controller tuning for Steering Control of Autonomous Underwater Vehicle: Genetic Algorithm Approach. In Proceedings of the 2016 Indian Control Conference (ICC), Hyderabad, India, 4–6 January 2016; pp. 335–340.
44. Farhan, M.F.; Shukor, N.S.A.; Ahmad, M.A.; Suid, M.H.; Ghazali, M.R.; Jusof, M.F.M. A simplify fuzzy logic controller design based safe experimentation dynamics for Pantograph-Cateary system. *Indones. J. Electr. Eng. Comput. Sci.* **2019**, *14*, 903–911. [CrossRef]
45. Abro, G.E.M.; Asirvadam, V.S.; Zulkifli, S.A. Single-Input Fuzzy-Sliding Mode Control for an Underactuated Quadrotor Craft. In Proceedings of the 2020 IEEE 2nd International Conference on Artificial Intelligence in Engineering and Technology (IICAIET), Kota Kinabalu, Malaysia, 26–27 September 2020; pp. 1–6.
46. Emran, B.J.; Najjaran, H. A review of quadrotor: An underactuated mechanical system. *Annu. Rev. Control* **2018**, *46*, 165–180. [CrossRef]
47. Asif, M.; Memon, A.Y.; Khan, M.J. Output Feedback Control for Trajectory Tracking of Wheeled Mobile Robot. *Intell. Autom. Soft Comput.* **2015**, *22*, 75–87. [CrossRef]
48. Abro, G.E.M.; Jabeen, B.; Manan, A. Stabilization of Non-holonomic 03 DOF Hovercraft using Robust RST Control Design. *Sukkur IBA J. Emerg. Technol.* **2019**, *2*, 45–50. [CrossRef]
49. Ali, Z.A.; Wang, D.; Masroor, S.; Loya, M.S. Attitude and Altitude Control of Trirotor UAV by Using Adaptive Hybrid Controller. *J. Control Sci. Eng.* **2016**, *2016*, 1–12. [CrossRef]
50. Lee, S.J.; Jang, I.; Kim, H.J. Fail-safe Flight of a Fully-Actuated Quadcopter in a Single Motor Failure. *arXiv* **2020**, arXiv:2002.11326.
51. Manouchehri, P.; Ghasemi, R.; Toloei, A. Distributed Fuzzy Adaptive Sliding Mode Formation for Nonlinear Multi-quadrotor Systems. *Int. J. Eng.* **2020**, *33*, 798–804.
52. Li, X.; Zhang, H.; Fan, W.; Zhao, J.; Wang, C. Multivariable finite-time composite control strategy based on immersion and invariance for quadrotor under mismatched disturbances. *Aerosp. Sci. Technol.* **2020**, *99*, 105763. [CrossRef]
53. Dantsker, O.D.; Marco, C.; Moiz, V.; Renato, M. Flight & Ground Testing Data Set for an Un-manned Aircraft: Great Planes Avistar Elite. In *AIAA Scitech 2020 Forum*; AIAA: Orlando, FL, USA, 2020; p. 0780.
54. Xiong, J.-J.; Zhang, G.-B. Global fast dynamic terminal sliding mode control for a quadrotor UAV. *ISA Trans.* **2017**, *66*, 233–240. [CrossRef] [PubMed]
55. Wu, B.; Chang, X.H.; Zhao, X. Fuzzy H∞ output feedback control for nonlinear NCSs with quantization and stochastic communication protocol. *IEEE Trans. Fuzzy Syst.* **2020**. [CrossRef]
56. Song, X.; Wang, M.; Ahn, C.K.; Song, S. Finite-Time H∞H∞ Asynchronous Control for Nonlinear Markov Jump Distributed Parameter Systems via Quantized Fuzzy Output-Feedback Approach. *IEEE Trans. Cybern.* **2020**, *50*, 4098–4109. [CrossRef] [PubMed]
57. Hoffmann, G.; Huang, H.; Waslander, S.; Tomlin, C. Quadrotor helicopter flight dynamics and control: Theory and experiment, in 'AIAA Guidance. In Proceedings of the Navigation and Control Conference and Exhibit, Hilton Head Boston, SC, USA, 20–23 August 2007; pp. 20–23.
58. Bristeau, P.-J.; Martin, P.; Salaun, E.; Petit, N. The role of propeller aerodynamics in the model of a quadrotor UAV. In Proceedings of the 2009 European Control Conference (ECC), Budapest, Hungary, 23–26 August 2009; pp. 683–688.
59. Yogianandh, N.; Riaan, S.; Glen, B. Development of an UAV for search and rescue applications. In Proceedings of the IEEE Africon 2011, Nairobi, Keny, 13–15 September 2011; pp. 993–998.
60. Patel, A.R.; Patel, M.A.; Vyas, D.R. Modeling and analysis of quadrotor using sliding mode control. In Proceedings of the 2012 44th Southeastern Symposium on System Theory (SSST), Jacksonville, FL, USA, 11–13 March 2012; pp. 111–114.
61. Zhan, Q.; Wang, J.; Xi, X. Control System Design and Experiments of a Quadrotor. In Proceedings of the 2012 IEEE International Conference on Robotics and Biomimetics (ROBIO), Guangzhou, China, 11–14 December 2012; Institute of Electrical and Electronics Engineers (IEEE): Guangzhou, China, 2012; pp. 1152–1157.
62. De Jesus Rubio, J.; Cruz, J.H.P.; Zamudio, Z.; Salinas, A.J. Comparison of two quadrotor dynamic models. *IEEE Lat. Am. Trans.* **2014**, *12*, 531–537. [CrossRef]
63. Bouabdallah, S.; Roland, S. Towards intelligent miniature flying robots. In *Field and Service Robotics*; Springer: Berlin/Heidelberg, Germany, 2006; pp. 429–440.
64. Alexis, K.; Tzes, A.; Nikolakopoulos, G. Model predictive quadrotor control: Attitude, altitude and position experimental studies. *IET Control Theory Appl.* **2012**, *6*, 1812–1827. [CrossRef]
65. Zadeh, L.A. *Fuzzy Logic Toolbox for Use with MATLAB*; The MathWorks Inc.: Natick, MA, USA, 1999.